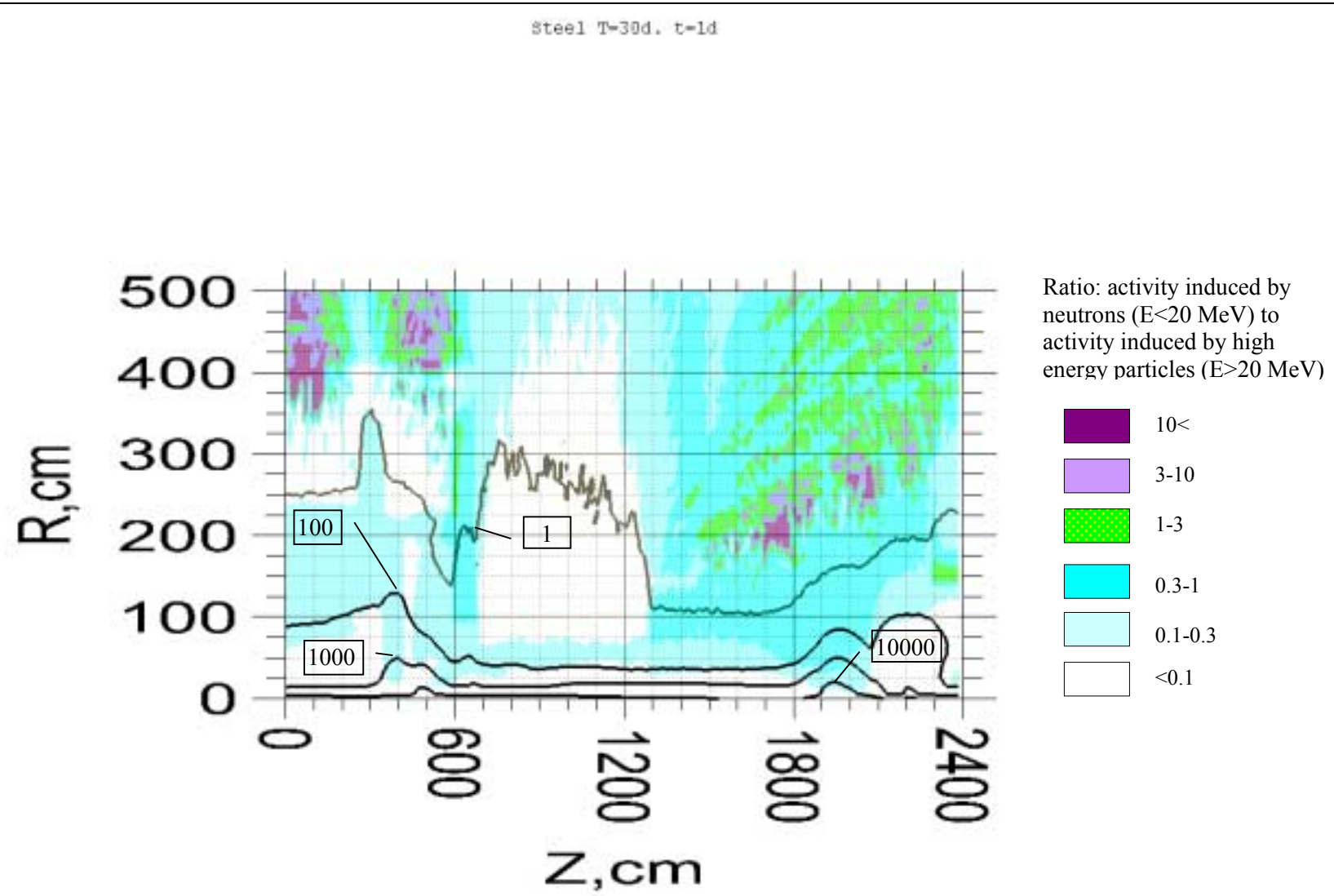

Fig .50. Distribution of induced radioactivity in Stainless Steel calculated at T=30d, t=1d. The levels show contact dose rate in μSv/h.

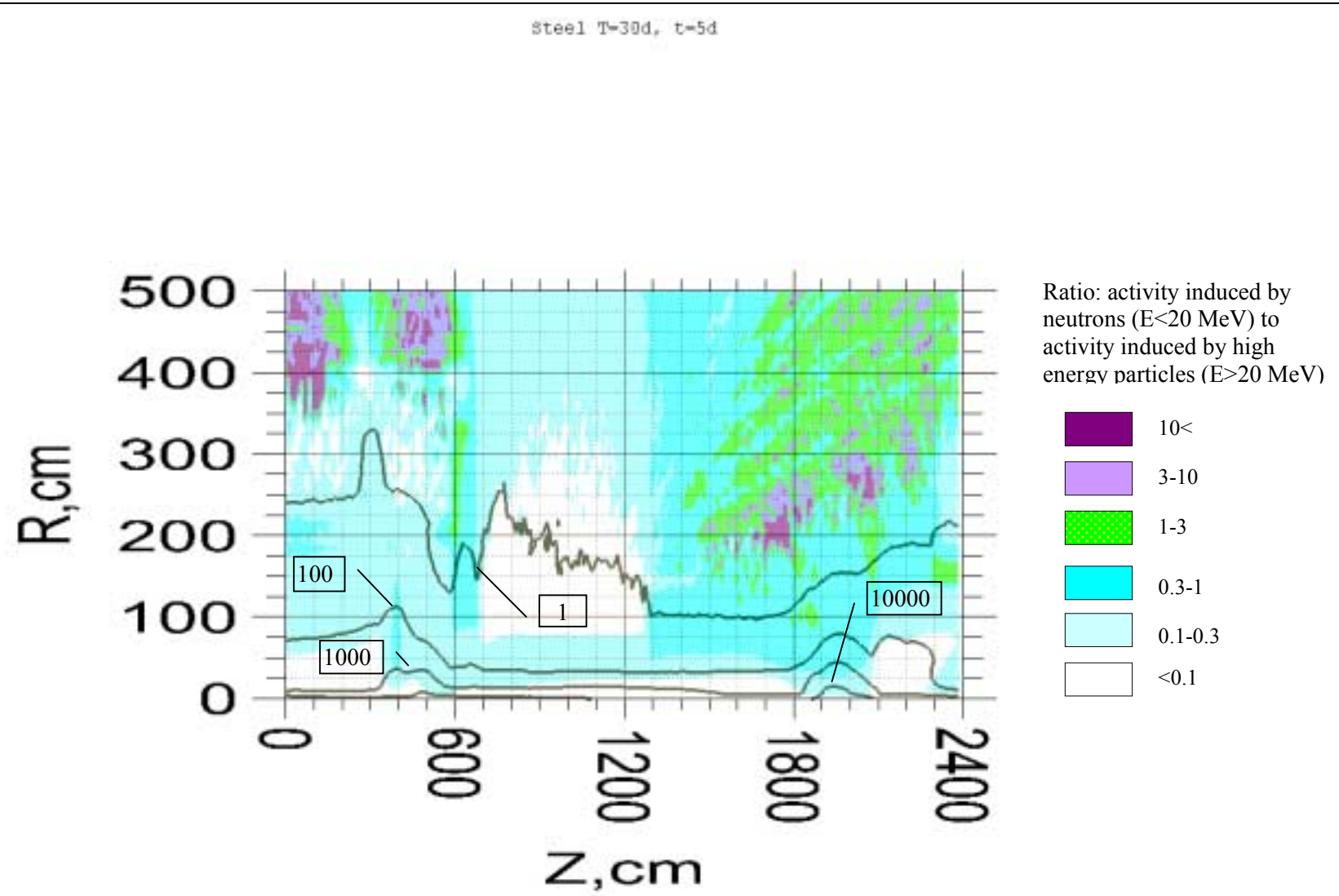

Fig .51. Distribution of induced radioactivity in Stainless Steel calculated at T=30d, t=5d. The levels show contact dose rate in μSv/h.

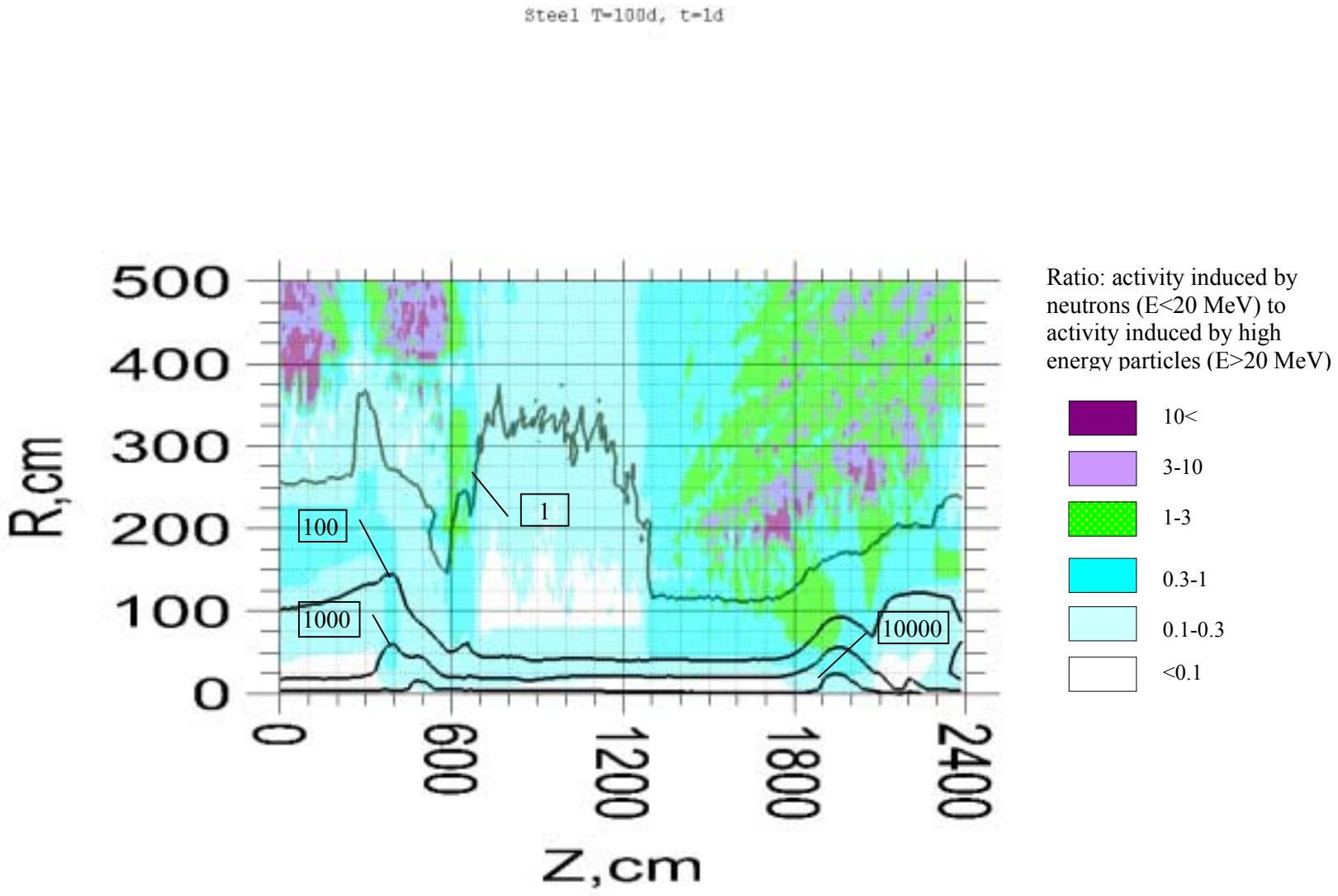

Fig .52. Distribution of induced radioactivity in Stainless Steel calculated at T=100d, t=1d. The levels show contact dose rate in μSv/h.

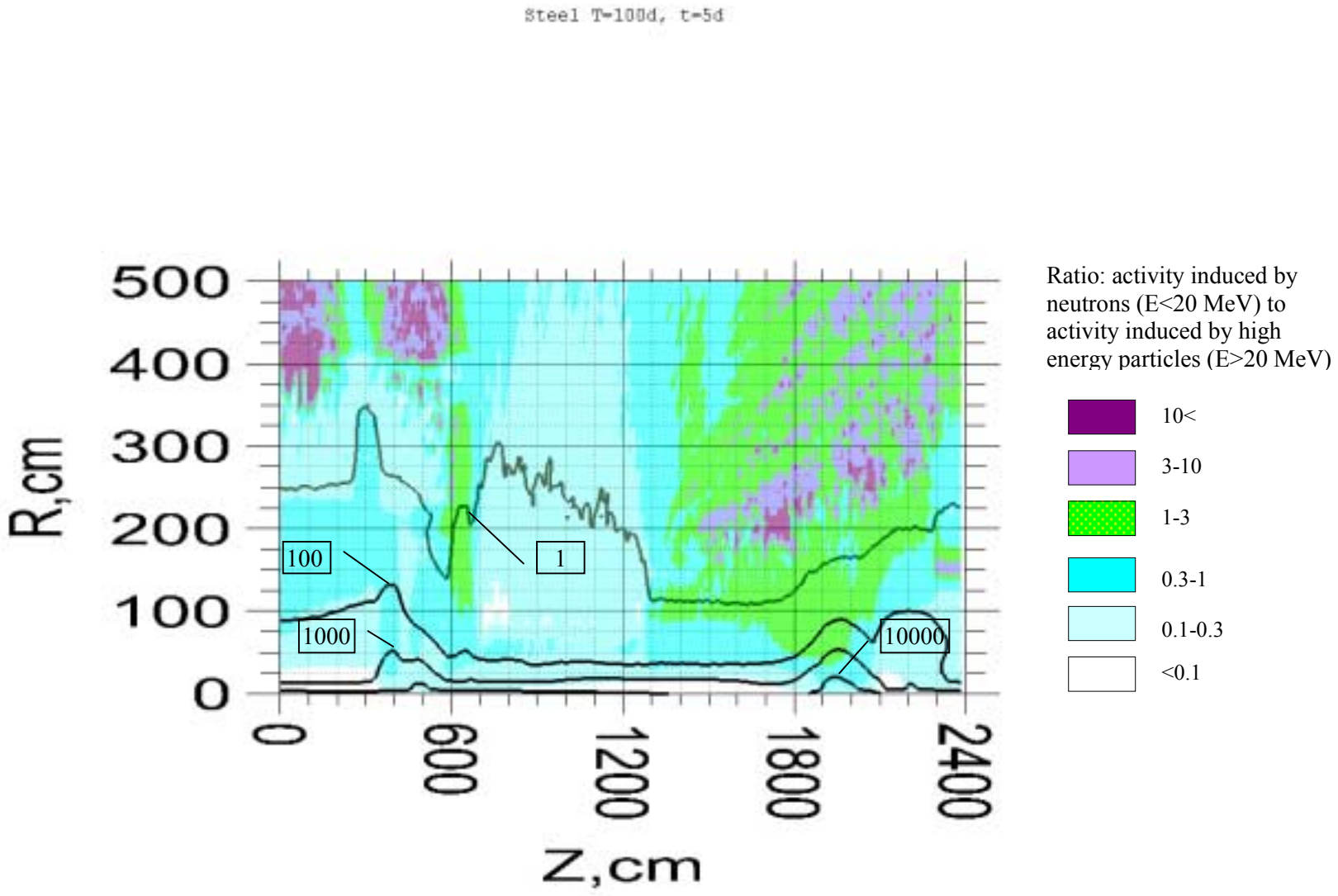

Fig .53. Distribution of induced radioactivity in Stainless Steel calculated at T=100d, t=5d. The levels show contact dose rate in μSv/h.

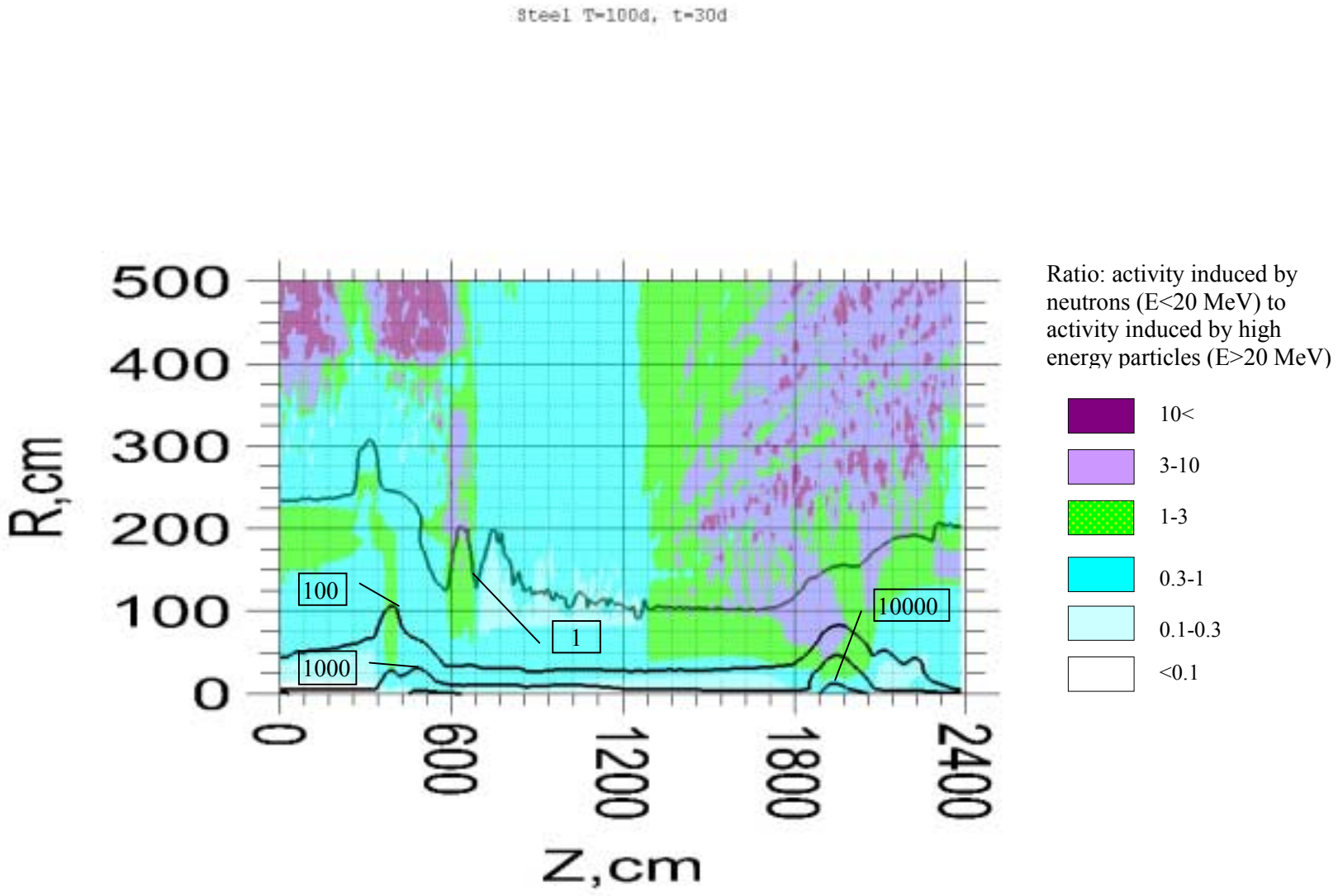

Fig .54. Distribution of induced radioactivity in Stainless Steel calculated at T=100d, t=30d. The levels show contact dose rate in μSv/h.

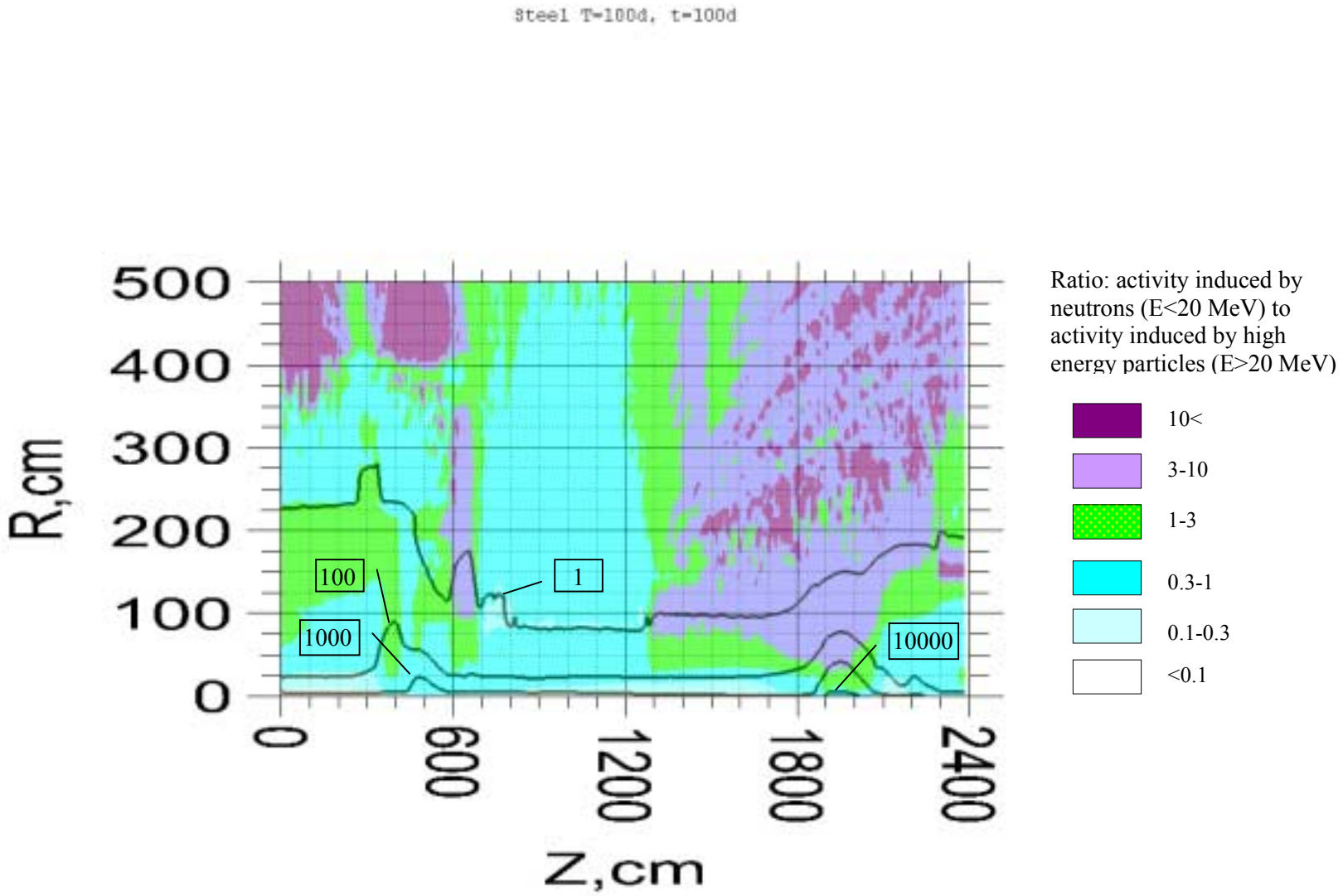

Fig .55. Distribution of induced radioactivity in Stainless Steel calculated at T=100d, t=100d. The levels show contact dose rate in μSv/h.

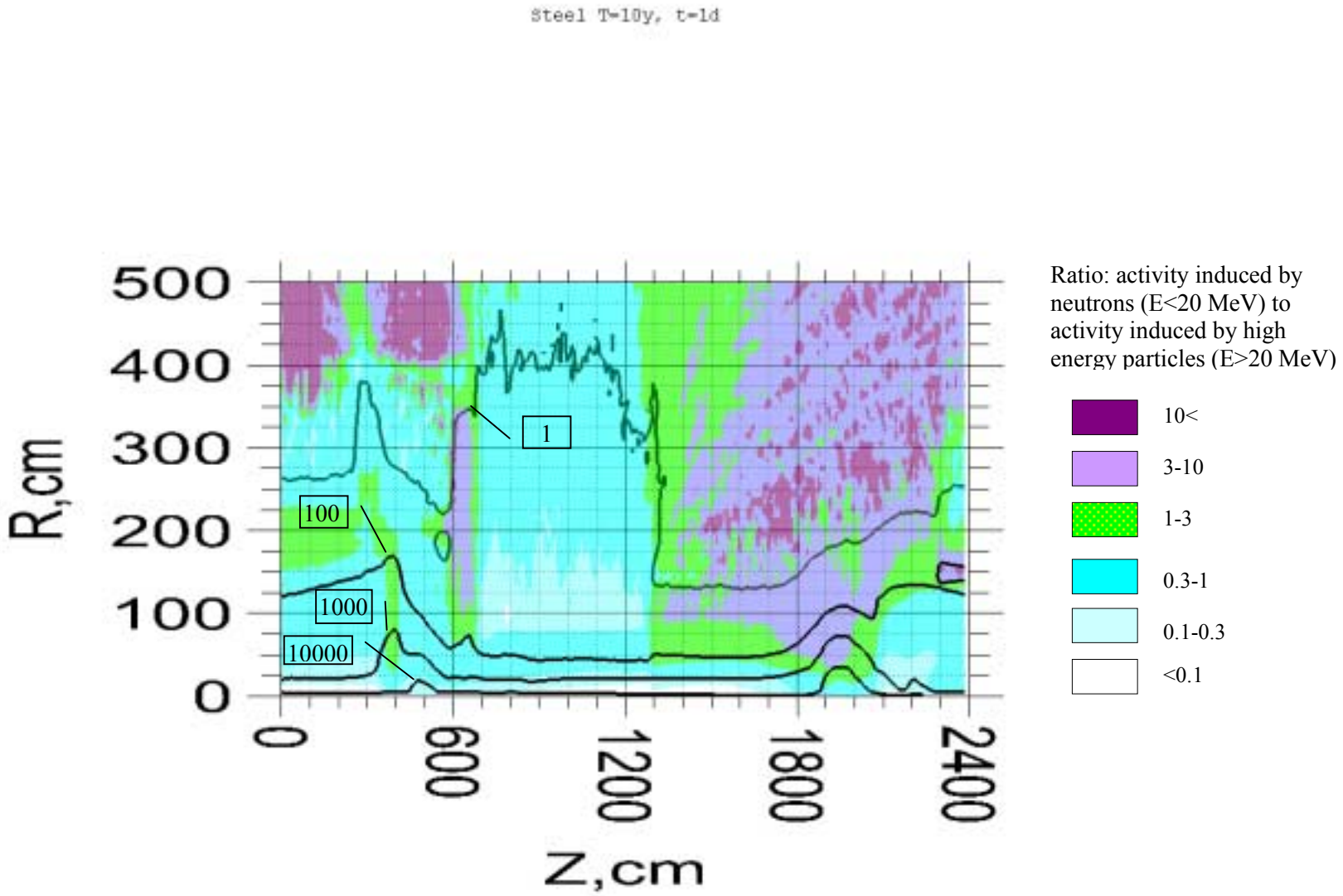

Fig .56. Distribution of induced radioactivity in Stainless Steel calculated at T=10y, t=1d. The levels show contact dose rate in μSv/h.

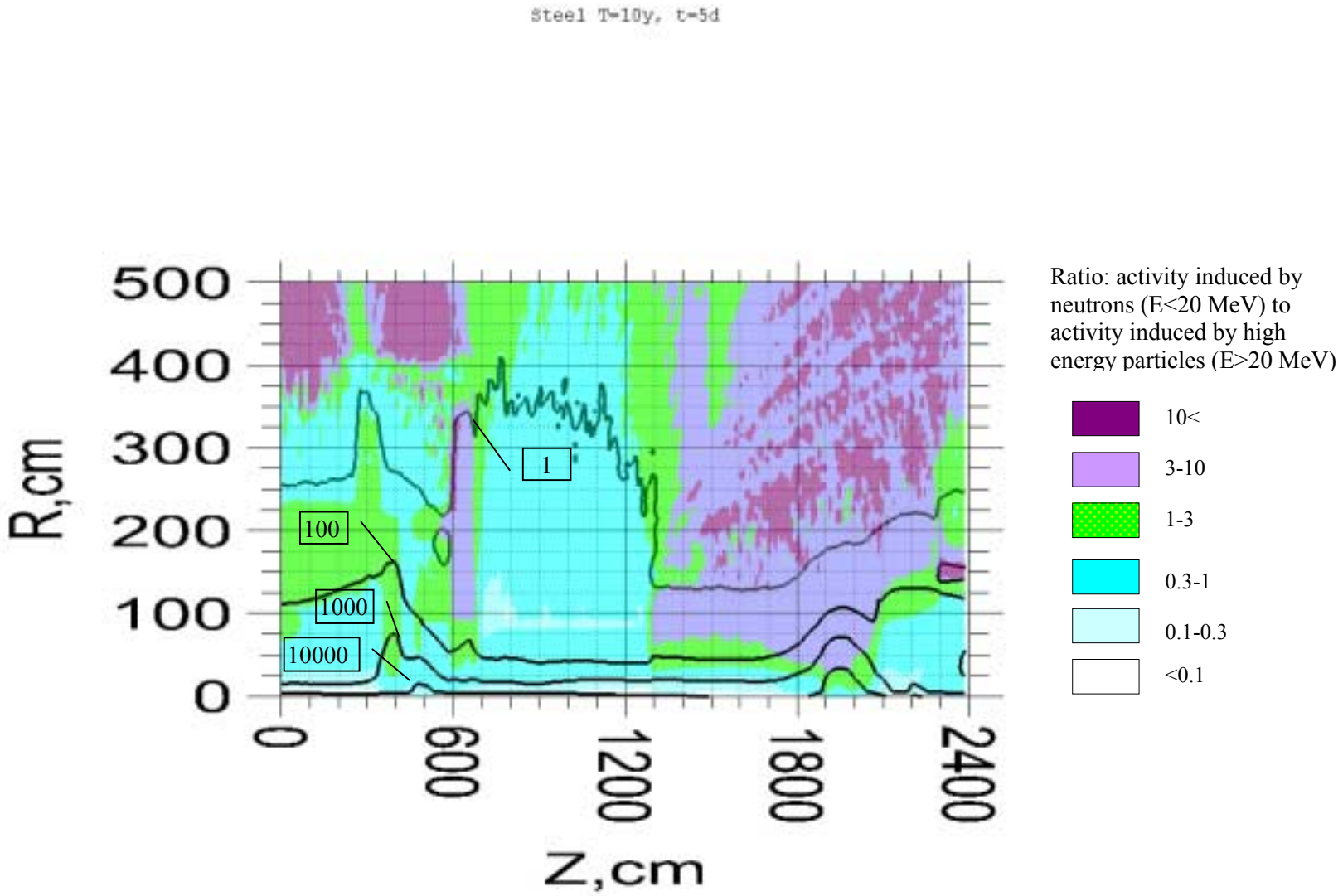

Fig .57. Distribution of induced radioactivity in Stainless Steel calculated at T=10y, t=5d. The levels show contact dose rate in μSv/h.

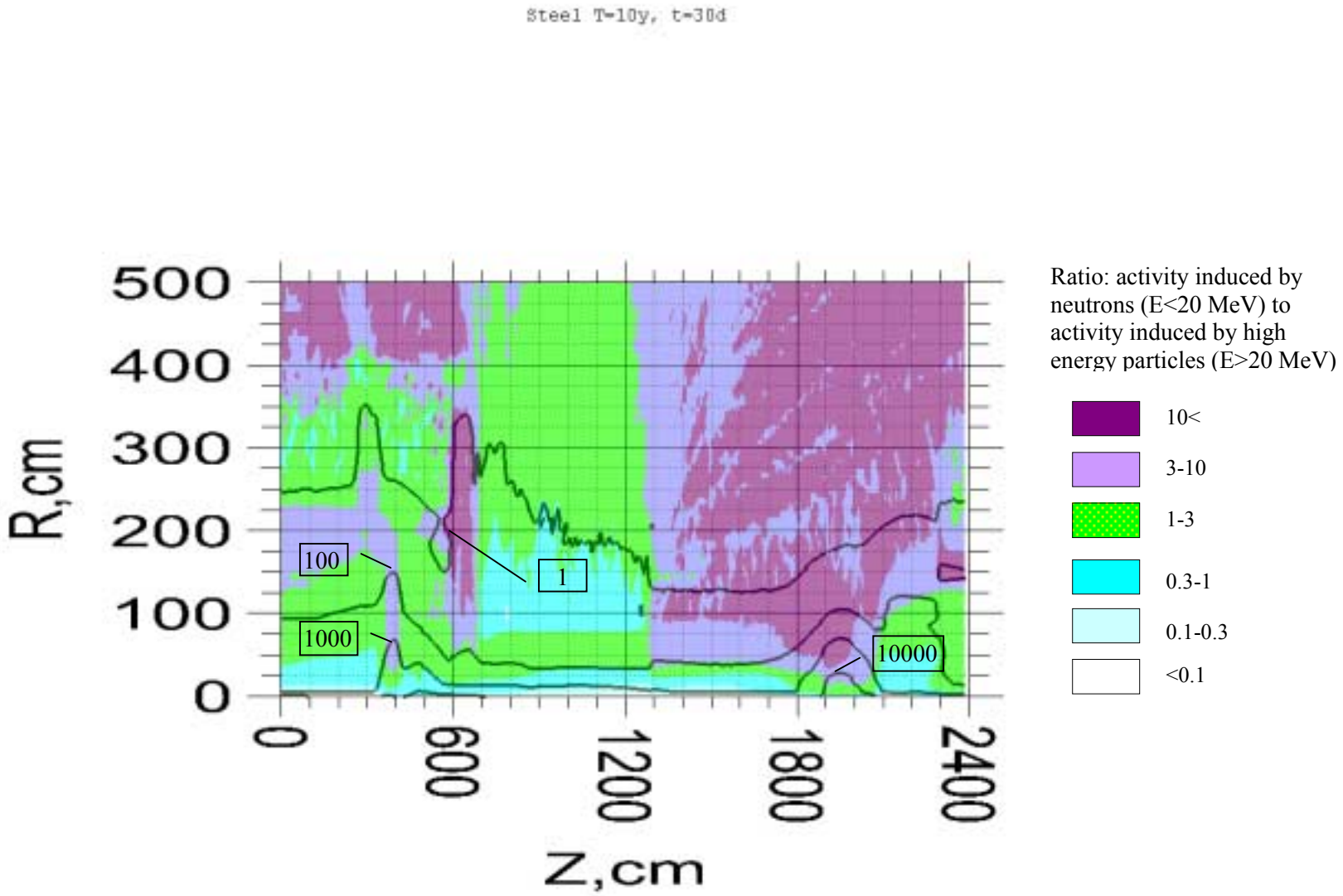

Fig .58. Distribution of induced radioactivity in Stainless Steel calculated at T=10y, t=30d. The levels show contact dose rate in μSv/h.

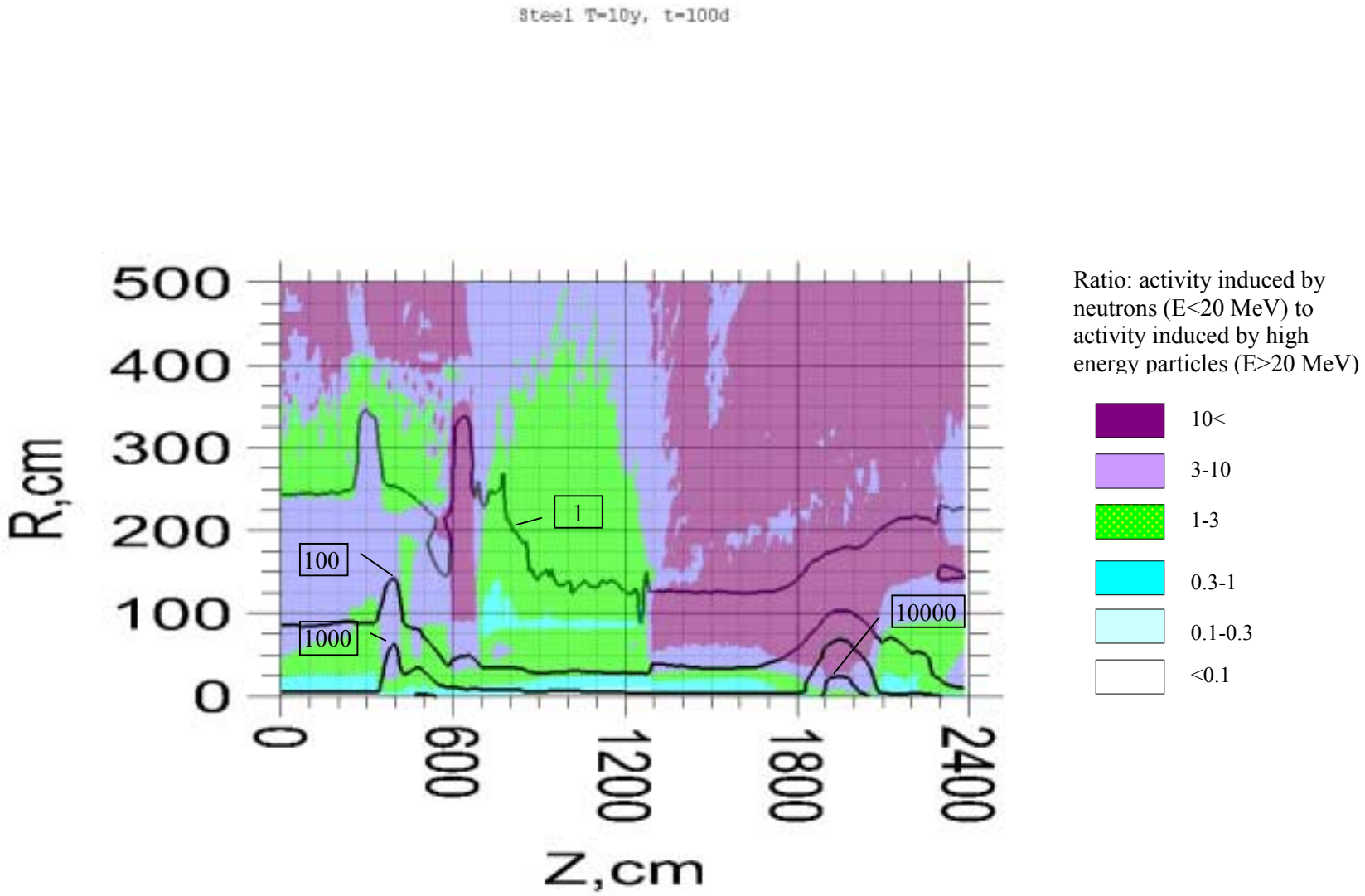

Fig .59. Distribution of induced radioactivity in Stainless Steel calculated at T=10y, t=100d. The levels show contact dose rate in μSv/h.

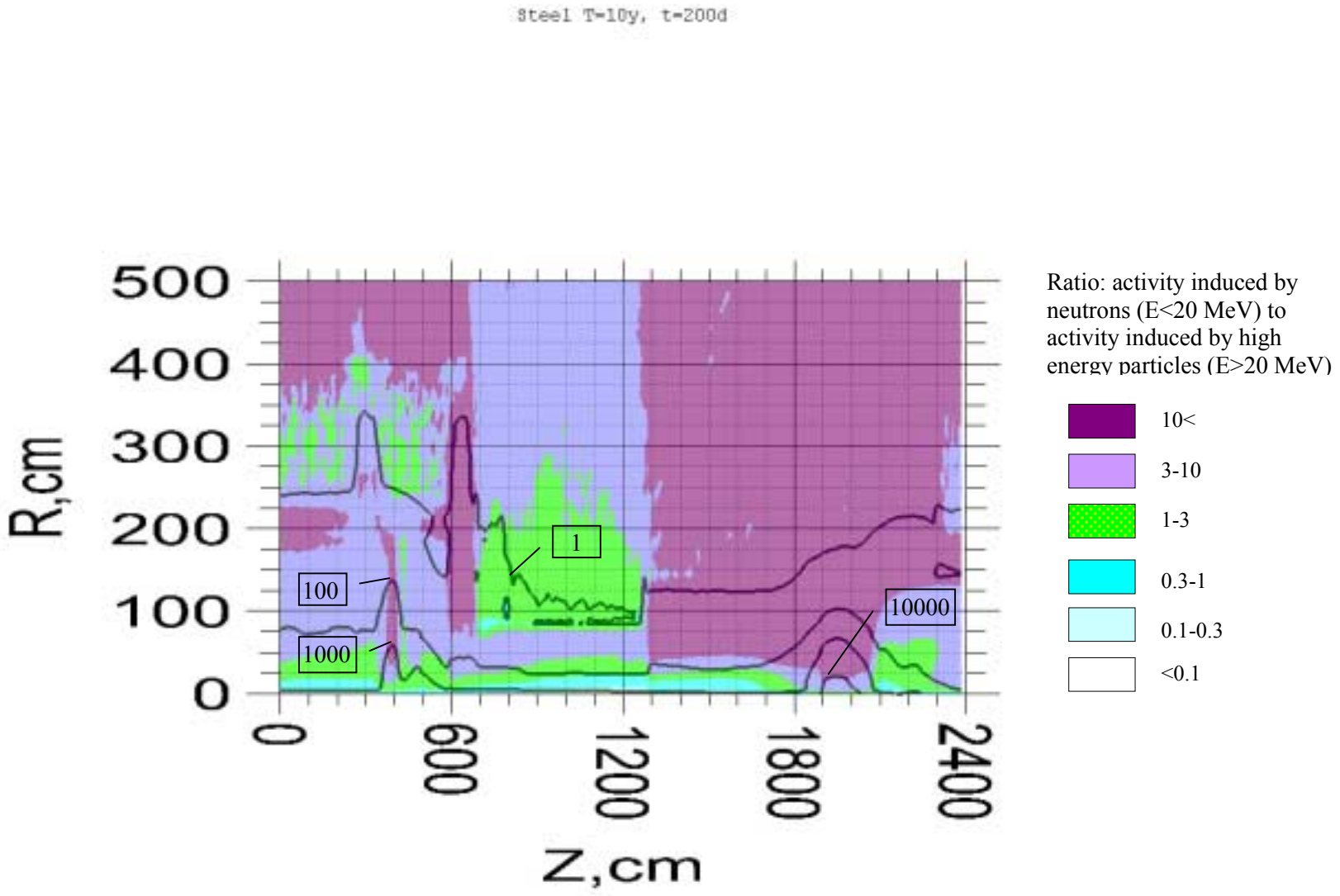

Fig .60. Distribution of induced radioactivity in Stainless Steel calculated at T=10y, t=200d. The levels show contact dose rate in μSv/h.

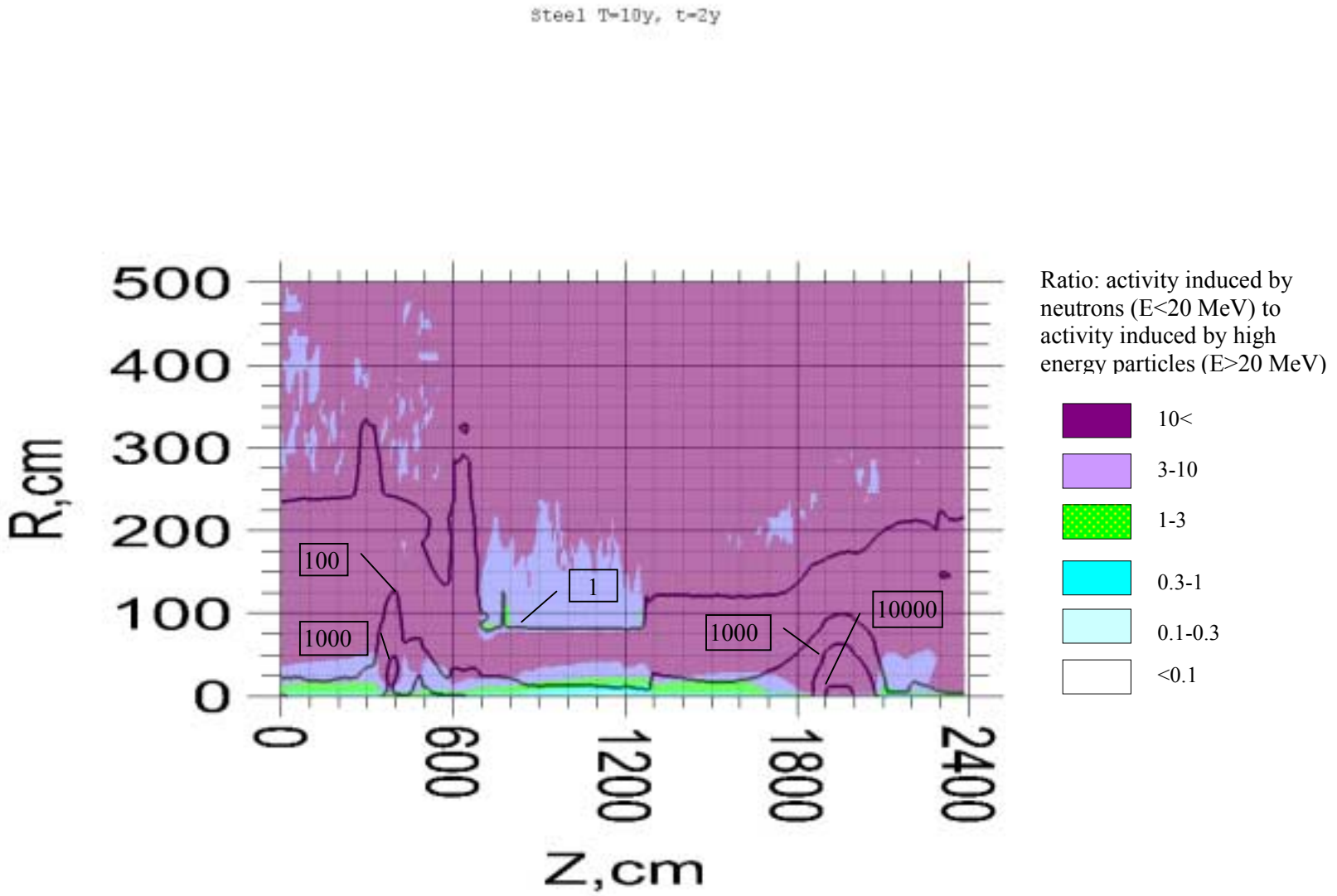

Fig .61. Distribution of induced radioactivity in Stainless Steel calculated at T=10y, t=2y. The levels show contact dose rate in μSv/h.